Numerical Analysis of a Damage Evolution in Adhesive Overlapping Metal/Fiber-Reinforced Polymer Structures

Natalia Konchakova, Ralf Mueller and Franz-Josef Barth*
Institute of Applied Mechanics, University of Kaiserslautern
P.O. Box 3049, D-67653 Kaiserslautern, Germany
e-mail: konchako@rhrk.uni-kl.de, ram@rhrk.uni-kl.de, barth@rhrk.uni-kl.de

Abstract

The damage evolution in light weight engineering structures, like aluminum/fiber-reinforced polymer specimens, is investigated. Joints of aluminium alloy 5754 (AA5754) and carbon fibre reinforced thermoplastic composite CF-PA66 are manufactured by means of an adhesion with an epoxy (1K-EP). The gluing zone is considered as an interface material. The aim of the research is to study the influence of the interface geometry on the mechanical characteristics of the structure. The finite element method is used for the simulation of the complex tensile joint. The aluminium substrate is modelled as an elasto-plastic continuum with linear (isotropic) hardening. The polymer composite possesses an orthotropic elastic behaviour. A viscoelastic model with the Lemaitre-type damage is applied to the adhesive interface material. A solid interface approach is used for the discretisation of the damage domain. It is shown that damage evolution depends on the geometry of the interface. The present work contains the numerical analysis of fracture process of the adhesive specimens with squared, rectangular-like and circle-shaped geometry of the interfacial joint.

Keywords: damage, finite element method, viscoelasticity, material properties

1. Introduction

Metal/polymer composite joints have a great potential for application in a large number of engineering sectors. These material systems are opening up new possibilities for innovative product developments in automotive and aerospace industries. The high specific stiffness and physico-chemical resistance of polymer composites are combined with traditional strength of metals in these advantageous combinations. The joints can be produced by ultrasonic metal welding or by means of adhesive bonding [1, 2]. The simulation of such modern engineering structures is economical important. The applications of a finite element method to analyze the mechanical behaviour of the light weight engineering structures, like aluminum/fiber-reinforced polymer specimens is known [3, 4]. In this contribution, the simulation of a single overlapping shear-tensile specimen with adhesive bonding is considered. The joints of aluminium alloy 5754 (AA5754) and carbon fibre reinforced thermoplastic composite CF-PA66 is realised by means of an adhesion with an epoxy. Solid interface approach is applied to simulate the gluing zone. It is considered as an interface material. So, there are three model parts in the specimen of the joint: the polymer composite (matrix and fibre reinforced), the metalic partner and an interface material in the joint adhesive zone.

2. Interfacial material model

A viscoelastic model with the Lemaitre-type damage is taken into account for the modelling of the properties of the interface adhesive material. The displacement jump $[\mathbf{u}]$ is split into an elastic part $[\mathbf{u}]^e$ and a viscous part $[\mathbf{u}]^{ve}$

$$[\mathbf{u}] = [\mathbf{u}]^e + [\mathbf{u}]^{ve}, \tag{1}$$

where $[\mathbf{u}] = \mathbf{u}_{\Gamma+} - \mathbf{u}_{\Gamma-}$ is the jump across the adhesive interface Γ. The tractions of the interface are derived from the free energy function of the interface $\Psi^{if} = \Psi^{if}\left([\mathbf{u}], [\mathbf{u}]^e, d_i\right)$:

$$\boldsymbol{\tau} = \frac{\partial \Psi^{if}}{\partial [\mathbf{u}]} + \frac{\partial \Psi^{if}}{\partial [\mathbf{u}]^e} = \boldsymbol{\tau}^{\boldsymbol{\infty}} + \boldsymbol{\tau}^{\boldsymbol{m}} \tag{2}$$

The first part of the interface traction $\boldsymbol{\tau}^{\boldsymbol{\infty}}$ is the traction of a parallel spring. The second part of the decomposition $\boldsymbol{\tau}^{\boldsymbol{m}}$ is the traction of a serial arrangement of a damper and a spring [5]. The dependencies of the tractions are given as

$$\begin{aligned} \boldsymbol{\tau}^{\boldsymbol{\infty}} &= \left[\sum_i \left[1 - d_i\right] \mathbf{C}_i^{if,el,\infty}\right] \cdot [\mathbf{u}], \\ \boldsymbol{\tau}^{\boldsymbol{m}} &= \left[\sum_i \left[1 - d_i\right] \mathbf{C}_i^{if,el,m}\right] \cdot [\mathbf{u}]^e, \qquad i = s,t,n, \end{aligned} \tag{3}$$

where $\{s,t,n\}$ are the orthonormal interfacial directions, the elastic interfacial tangent stiffness tensor with respect to the parallel spring is $\mathbf{C}_i^{if,el,\infty}$ and to the damper system spring is $\mathbf{C}_i^{if,el,m}$. The damage parameter d_i is introduced, with $d_i \in [0,1[$ and $\dot{d}_i > 0$, thus healing effects are excluded. It is incorporated in a Lemaitre-type damage context [6]. For $d_i \to 1$, the material tends to be fully damaged and unable to bear any load. Exponential relations are chosen for the damage parameter:

$$d_i = 1 - \exp(j_i[\mu_{i(0)} - \mu_i]). \tag{4}$$

The variable μ_i accounts for the progression of damage in $i-$direction. It is computed according to

$$\mu_i = \max\left(\bar{\mu}_i([\mathbf{u}], [\mathbf{u}]^e), \mu_{i(0)}\right)$$

and the so-called damage driving force is given by

$$\bar{\mu}_i = -\frac{\partial \Psi^{if}}{\partial d_i}.$$

*The authors thank the German Research Foundation (DFG) for the financial support within the Research Unit (FOR) 524 "Manufacturing, Characterisation and Simulation of Welded Lightweight Structures of Metal/Fibre-reinforced Polymer Composites" at the University of Kaiserslautern.

The constitutive assumption of viscoelasticity is given by the rate dependency

$$\dot{[u_i]}^{ve} = \frac{\tau_i^m}{\eta_i} = \frac{1-d_i}{T_i}\left[[u_i]-[u_i]^{ve}\right], \quad T_i = \frac{\eta_i}{c_i^m} \tag{5}$$

where η_i denotes to the viscosity in i-direction, T_i is the relaxation time.

3. Computation of bulk materials

The material AA5754 is simulated as a elastoplastic material with isotropic hardening. The polymer composite CF-PA66 generally shows an orthotropic elastic behaviour.

3.1. Elastoplastic model with isotropic hardening

An elastoplastic bulk material law with isotropic hardening is used to model the aluminium plate [3, 4]. The total strain $\boldsymbol{\varepsilon}$ is split by

$$\boldsymbol{\varepsilon} = \boldsymbol{\varepsilon}^e + \boldsymbol{\varepsilon}^p \tag{6}$$

into an elastic part $\boldsymbol{\varepsilon}^e$ and a plastic part $\boldsymbol{\varepsilon}^p$. Stresses are given as

$$\boldsymbol{\sigma} = \boldsymbol{\sigma}(\boldsymbol{\varepsilon}^e, \alpha^p) \tag{7}$$

depending on the elastic strains and a plastic parameter α^p, accounting for irreversible plastic effects. In order to separate an elastic and a plastic range for loads above the yield limit, the von Mises yield function is proposed as

$$\Phi = \sqrt{\frac{3}{2}}|\boldsymbol{\sigma}^{dev}| - [Y_0 + H^p\alpha^p], \tag{8}$$

where Y_0 is initial the yield stress, H^p is a hardening modulus, $\boldsymbol{\sigma}^{dev}$ is the deviatoric part of the stress tensor.

3.2. Orthotropic elastic model

The orthotropic linear elastic model with two orthogonal directions of anisotropy $\boldsymbol{e_1}$ and $\boldsymbol{e_2}$ is applied for the computation of a second bulk material. So, two corresponding structure tensors $\boldsymbol{A_1} = \boldsymbol{e_1}\otimes\boldsymbol{e_1}$ and $\boldsymbol{A_2} = \boldsymbol{e_2}\otimes\boldsymbol{e_2}$ are introduced. In this case the free energy can be represented with regard to 7 invariants [5]:

$$\Psi = \Psi\left(i_\varepsilon, i_{\varepsilon A_1}, i_{\varepsilon A_2}\right) = \Psi\left(I_1, I_2, I_3, I_4, I_5, I_6, I_7\right).$$

Where $i_\varepsilon = \{I_1, I_2, I_3\}$, $i_{\varepsilon A_1} = \{I_4, I_5\} = \{\varepsilon : \boldsymbol{A_1}, \varepsilon^2 : \boldsymbol{A_1}\}$, $i_{\varepsilon A_2} = \{I_6, I_7\} = \{\varepsilon : \boldsymbol{A_2}, \varepsilon^2 : \boldsymbol{A_2}\}$.

The stresses are computed by differentiating the free energy with respect to the invariants:

$$\begin{aligned}\boldsymbol{\sigma} = \frac{\partial\Psi}{\partial\boldsymbol{\varepsilon}} =& \Phi_1\,\mathbf{I} + \Phi_2\,\boldsymbol{\varepsilon} + \Phi_3\,\boldsymbol{\varepsilon}^2 + \Phi_4\,\mathbf{A_1} + \\ & \Phi_5\,2\,[\boldsymbol{\varepsilon}\cdot\mathbf{A_1}]^{sym} + \Phi_6\,\mathbf{A_2} + \Phi_7\,2\,[\boldsymbol{\varepsilon}\cdot\mathbf{A_2}]^{sym}.\end{aligned}$$

Here $\Phi_1 = \partial\Psi/\partial I_1 = \lambda\, I_1 + \alpha_1\, I_4 + \alpha_2\, I_6$,
$\Phi_2 = \partial\Psi/\partial I_2 = 2\mu$,
$\Phi_3 = \partial\Psi/\partial I_3 = 0$,
$\Phi_4 = \partial\Psi/\partial I_4 = \alpha_1\, I_1 + \beta_1\, I_4 + \beta_3\, I_6$,
$\Phi_5 = \partial\Psi/\partial I_5 = 2\mu_1$,
$\Phi_6 = \partial\Psi/\partial I_6 = \alpha_2\, I_1 + \beta_3\, I_4 + \beta_2\, I_6$,
$\Phi_7 = \partial\Psi/\partial I_7 = 2\mu_2$;
$\lambda, \mu, \alpha_i, \mu_i$ and β_i are orthotropic material parameters;
$\mathbf{I} = \delta_{ij}\boldsymbol{e_i}\otimes\boldsymbol{e_j}$ is the identity tensor.

4. Numerical simulation

The finite element method is used to simulate tensile joints. The bulk materials are computed by means of standard continuum elements. The adhesive zone is modelled with a solid interface approach by using special interface elements. Solid interfaces are one geometrical dimension lower than the surrounding continuum [5]. Thus, to model interfaces in three dimensions, two dimensional interface elements are needed. For the determination of the displacements $\mathbf{u}$ and the displacement jumps $[\mathbf{u}]$ across the interface the principle of virtual work with virtual displacements $\hat{\mathbf{u}}$ and $[\hat{\mathbf{u}}]$ is used. The finite element approximation of the displacement jump and the test function jump [5] are given by

$$[\mathbf{u}]^h(\xi_1,\xi_2) = \mathbf{B}_{el}\cdot\mathbf{u}^N, \quad [\hat{\mathbf{u}}]^h(\xi_1,\xi_2) = \mathbf{B}_{el}\cdot\hat{\mathbf{u}}^N,$$

where $\mathbf{u}^N = [\mathbf{u}_1,\mathbf{u}_2,\mathbf{u}_3,\mathbf{u}_4,\mathbf{u}_5,\mathbf{u}_6,\mathbf{u}_7,\mathbf{u}_8]^T$ and $\hat{\mathbf{u}}^N = [\hat{\mathbf{u}}_1,\hat{\mathbf{u}}_2,\hat{\mathbf{u}}_3,\hat{\mathbf{u}}_4,\hat{\mathbf{u}}_5,\hat{\mathbf{u}}_6,\hat{\mathbf{u}}_7,\hat{\mathbf{u}}_8]^T$ are the nodal displacements of the adjacent elements. The matrix $\mathbf{B}_{el}$ is the element operator matrix. The ansatz functions for the interface elements are introduced by

$$N_N(\xi_1,\xi_2) = \frac{1}{4}[1+\xi_{1N}\xi_1][1+\xi_{2N}\xi_2],$$

where the index N denotes the number of the node and ξ_{1N}, ξ_{2N} are the nodal coordinates in the element coordinate system. The interpolation variables are given by $\xi_1, \xi_2 \in [-1, 1]$.

5. Results and Discussion

The influence of interface geometry on the mechanical characteristics of adhesived overlapping tensile specimen is analysed. Three different geometries of adhesive interfaces are considered: squared, circle-shaped and rectangular-like geometry, which correspond to the coupling faces. All three interface geometries have the same area of 100mm^2 and are placed in the centre of the overlapping zone (see Figure 1).

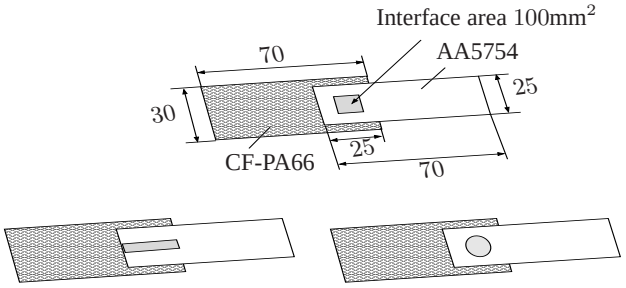

Figure 1: Geometry of adhesive AA5754/CF-PA66 joints

The material constants of AA5754 and CF-PA66 have been described in [3, 4] and are shown in Table1.The adhesive interfacial material parameters are: Young's Modulus $E = 1700$ [MPa], a viscosity $\eta_s = \eta_t = 319,55$[MPa s], $\eta_n = 850$[MPa s], a damage threshold in i-direction $\mu_{i(0)} = 38\cdot10^{-2}$[MPa m], an intensity of damage evolution $j_i = 23,5\cdot10^{-2}$[MPa m]$^{-1}$, $i = s, n, t$. The free and remote part of a polymer composite CF-PA66 is clamped. The free (non-adhesived) part of a AA5754 metal sheet is subjected to an extension. The given displacement is $|u_x^0| = 0.02$mm at each loadstep. We modeled the joint of aluminum sheet in a thickness of 1mm and also consolidated sheet of carbon fiber-reinforced polyamide 66 with a thickness of 2mm. Size of the adhesive square is 10mm×10mm, size of rectangles 25mm×4mm, the circle has a radius of $5,64$mm. In case of the square interface model, 3108 bulk and 100 interface elements are used. In case of an extended (elongated) rectangle, the model contains 3644 elements, including 160 interface elements. The third simulation for the circle-shaped interface uses 3834 elements, 140 are in the interface layer.

The numerical analysis of the lightwight strictures is based on the investigation of force-displacement relations. Figure 2 contains three simulated force-displacement curves of

Table 1: Mechanical properties of aluminum alloy sheet and the orthotropic parameters of carbon fiber reinforced polymer

AA5754				CF-PA66, [MPa]								
Young's Modulus [GPa]	Yield Strength [MPa]	Ultimate Tensile Strength [MPa]	Ultimate Strain [%]	λ	α_1	α_2	β_1	β_2	β_3	μ	μ_1	μ_2
70,58	177	250	13.5	4555	-3263	-3263	51466	51466	7524	-1000	1900	1900

aluminum/fiber-reinforced polymer tensile joints. We can observe from the graphs the region of viscoelastic behaviour, the zone of plastic flow and a damage response for all three geometries. Secondly, the state of specimens with square and rectangle interface is reflected by a rather similar behaviour of the force-displacement curves in all the three typical zones. As we can conclude from the graphs, the level of maximal loading is the same for all three joints, but the damage influence is first identified in the specimen with square interface. Fracture domain develops more actively in this specimen in comparison with the other two geometries.

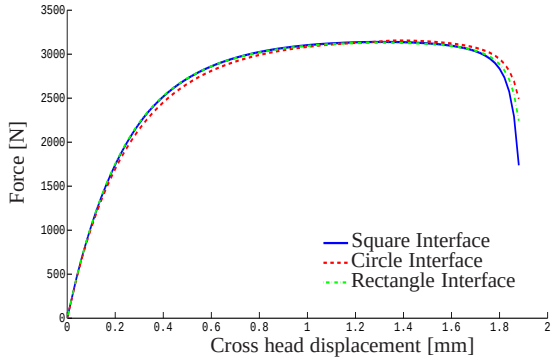

Figure 2: Force-displacement curves of adhesive AA5754/CF-PA66 joints

The state of interface in each loading zone can be analysed with help of interfaceal traction behaviour. The direction of the interface local coordinate system $\{s, t, n\}$ is different with nodal position of the interface elements. Therefore we analyze the distribution of the interface mechanical parameters in the whole welding area. The traction vector in the join surface can be computed by means of the following form:

$$\tau_{st} = \sqrt{\tau_s^2 + \tau_t^2}.$$

The numerical analysis of the maximal value of τ_{st} in the adhesive areas shows an increase of the traction in all interfaces for u$\in$ [0mm; 1, 4mm] for square and rectangle joints and u$\in$ [0mm; 1, 54mm] for circle geometry. In the next corresponding areas of displacement changing the tractions decrease.

The traction is the highest in circle interface and minimal in square interface on the each loadstep. However the interval of the traction growth is wider for circle geometry: the traction achieves it's highest value of $\sim$ 32[MPa] for u$\simeq$ 1, 26mm. The circle interface holds this traction approximately next 30 loadsteps until u$\simeq$ 1, 86mm. After that the τ_{st} function decreases quickly.

At the same time the joint with square interface has the area of high traction $\sim$ 27[MPa] while u$\in$ [1, 24mm; 1, 5mm]. Then we observe the falling of the τ_{st} function.

Figure 3 shows the distribution of the traction value τ_{st} in the adhesive surface for u= 1, 5mm. The zone of maximal traction is placed in the centre of interface. It is the state of the beginning of fracture. More than 80% of interface area has the maximal value of τ_{st}. At the next loadstep the function of τ_{st} decreases.

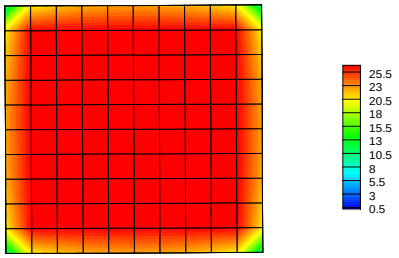

Figure 3: Distribution of traction τ_{st} in square joint area, u=1, 5mm

Figure 4 contains the distribution of the traction value τ_{st} in the circle surface for the same step of the loading - u=1, 5mm. As it is obvious from the graph, the peak traction value occurs in the central boundary part of the interface in the direction of loading. The state of the specimen is the state of plastic deformation. Further loading initiates the development and expansion of the region of maximal traction into the center of the interface.

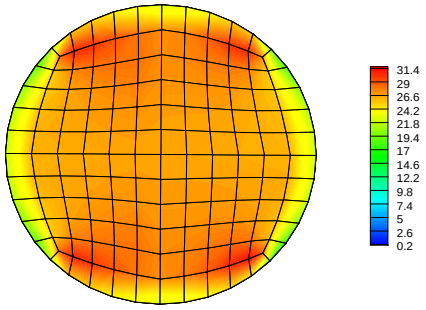

Figure 4: Distribution of traction τ_{st} in circle joint area, u=1, 5mm

The failure evolves into the joint area due to the action of a shear stress. At the initiale stage of damage evolution, with u$\in$ [0, 4mm; 0, 8mm], a shear stress in the joints initiates the formation of a zone of high damage at the boundary areas in the loading direction. An increase of the shear stress causes the growth of the damage zone into the center of the interface. Further loading contributes to the development and expansion of the

region of high damage into the interface. The maximal damage value

$$d_{st} = max\left(\sqrt{d_s^2 + d_t^2}\right)$$

in joint area is presented in Figure 5. The diagram consists of the measures of d_{st} for square and circle interfaces when cross head displacements equal $0,6$mm, $1,4$mm, $1,8$mm and $2,0$mm. As it is following from the figure, the maximal damage value develops rather similar in initiate stage of the loading. The damage value is approximately $0,2$ for both cases in the area of viscoelastic behaviour and about $0,32$ in the area of irreversible strain. The formation of failure domain is reflected of damage parameter increase when u$\geq 1,6$mm. The growth of the damage d_{st} in the corresponding area is more than $0,52$ for the case of circular geometry and $0,57$ in square interface. The increase of the damage values in the fracture zone (u$\geq 1,9$mm) is higher than $0,88$ in the case of square interface and $0,77$ in circle joint. With further loading, the values d_{st} grow. The region of maximum damage is located in the central part of the joint's overlap.

The distribution of d_{st} in the rectangle interface is between the corresponding value of damage in square and circle geometries. In all three cases, the value of d_{st} increases steadily with the increase of u. We can observe the formation of fracture domain when both of damage parts (d_s or d_t) tend to 1 for all three specimen.

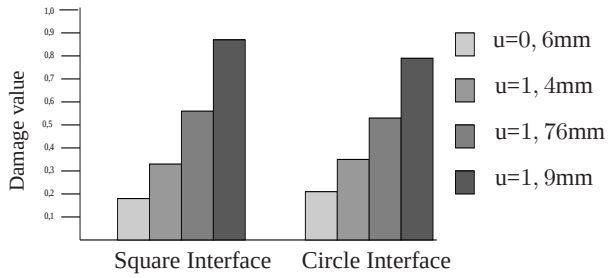

Figure 5: Maximal damage value d_{st} in joint area

So, the fracture develops more actively in the specimen with square interface geometry in comparison with the other two geometries. The damage in the adhesive domain evolves a bit slower in the case of rectangle geometry, and rather lazily in the circle-like joint. The difference between the damage values in the case of square and circle-like geometry is $\sim 11,01\%$ at the 100^{th} loadstep (when $u = 2,0$mm). Therefore, the numerical analysis of the damage evolution in the glued domain shows that damage evolves slower in the case of circular geometry.

6. Conclusion

The investigation of the mechanical properties of adhesive lightweight joints from aluminum alloy and fiber-reinforced polymer is based on the application of the viscoelastic model with Lemaitre-type damage and the solid interface approach. The phenomenological modelling of the interface characteristics allows us to compute successfully the global force-displacement curves for adhesive joints with different interface geometries. Three characteristics of the mechanical behavior of the specimen are observed and analyzed for all the geometries: the region of viscoelastic behavior, the plastic zone and the damage domain. We have observed a direct dependence of numerical values of the specimen's mechanical behavior on the adhesived geometry. Numerical analysis of the distribution of a interfacial traction and damage values shows that the specimen with a square interfacial area has the highest damage activity. The joint with circle like joint area can support high loading as compared to other geometries under consideration.

References

[1] Balle, F., Wagner, G., Eifler, D., Ultrasonic Metal Welding of Aluminium Sheets to Carbon Fibre Reinforced Thermoplastic Composites, *Advanced Engineering Materials*, 11, pp. 35-39, 2009.

[2] Velthuis, R., Koetter, M.P., Geiss, P.L., Mitschang, P., Schlarb A.K., Lightweight Structures Made of Metal and Fiber-Reinforced Polymers, *Kunststoffe international*, 11, pp. 22-24, 2007.

[3] Utzinger, J., Bos, M., Floeck,M., Menzel, A., Kuhl, E., Renz, R., Friedrich, K., Schlarb, A. and Steinmann, P., Computational modelling of thermal impact welded peek/steel single lap tensile specimens, *Int. J. Comput. Mater. Sci.*, 41, pp. 287-296, 2008.

[4] Konchakova, N., Balle, F., Barth,F.J., Mueller, R., Eifler, D., Steinmann, P., Finite Element Analysis of an Inelastic Interface in Ultrasonic Welded Metal/Fibre-Reinforced Polymer Joints, *Int. J. Comput. Mater. Sci*, 50, pp. 184-190, 2010.

[5] Utzinger, J., Analysis and Computation of Solid Interfaces on the Meso Scale, PhD thesis, TU Kaiserslautern, Germany, 2008.

[6] Lemaitre, J., *A Course on Damage Mechanics*, Springer, 1994.